

## The developing premature infant gut microbiome is a major factor shaping the microbiome of neonatal intensive care unit rooms

Brandon Brooks<sup>1</sup>, Matthew R. Olm<sup>1</sup>, Brian A. Firek<sup>2</sup>, Robyn Baker<sup>3</sup>, David Geller-McGrath<sup>4</sup>, Sophia R. Reimer<sup>4</sup>, Karina R. Soenjoyo<sup>4</sup>, Jennifer S. Yip<sup>4</sup>, Dylan Dahan<sup>5,6</sup>, Brian C. Thomas<sup>4</sup>, Michael J. Morowitz<sup>2</sup>, Jillian F. Banfield<sup>4\*</sup>

1 – Department of Plant and Microbial Biology, University of California, Berkeley, CA

2 – University of Pittsburgh School of Medicine, Pittsburgh, PA

3 – Division of Newborn Medicine, Children's Hospital of Pittsburgh of UPMC, Pittsburgh, PA

4 – Department of Earth and Planetary Sciences, University of California, Berkeley, CA

5 – Department of Biology, Bard College, Annandale-on-Hudson, NY, USA

6 – Department of Microbiology and Immunology, Stanford University School of Medicine, Stanford, CA, USA (current location)

\* corresponding author: [jbanfield@berkeley.edu](mailto:jbanfield@berkeley.edu)

18 **1.1 Abstract**

19  
20 Background: The neonatal intensive care unit (NICU) contains a unique cohort of patients with  
21 underdeveloped immune systems and nascent microbiome communities. Patients often spend  
22 several months in the same room and it has been previously shown that the gut microbiomes of  
23 these infants often resemble the microbes found in the NICU. Little is known, however, about the  
24 identity, persistence and absolute abundance of NICU room-associated bacteria over long stretches  
25 of time. Here we couple droplet digital PCR (ddPCR), 16S rRNA gene surveys, and recently  
26 published metagenomics data from infant gut samples to infer the extent to which the NICU  
27 microbiome is shaped by its room occupants.

28 Results: Over 2,832 swabs, wipes, and air samples were collected from sixteen private-style NICU  
29 rooms housing very low birthweight (<1,500 g), premature (<31 weeks' gestation) infants. For  
30 each infant, room samples were collected daily, Monday through Friday, for one month. The first  
31 samples from the first infant and last samples from the last infant were collected 383 days apart.  
32 Twenty-two NICU locations spanning room surfaces, hands, electronics, sink basins, and air were  
33 collected. Results point to an incredibly simple room community where 5-10 taxa, mostly skin  
34 associated, account for over 50% of 16S reads. Biomass estimates reveal 4-5 orders of magnitude  
35 difference between the least to the most dense microbial communities, air and sink basins,  
36 respectively. Biomass trends from bioaerosol samples and petri dish dust collectors suggest  
37 occupancy to be a main driver of suspended biological particles within the NICU. Using a machine  
38 learning algorithm to classify the origin of room samples, we show that each room has a unique  
39 microbial fingerprint. Several important taxa driving this model were dominant gut colonizers of  
40 infants housed within each room.

41 Conclusions: Despite regular cleaning of hospital surfaces, bacterial biomass was detectable at  
42 varying densities. A room specific microbiome signature was detected, suggesting microbes  
43 seeding NICU surfaces are sourced from reservoirs within the room and that these reservoirs  
44 contain actively dividing cells. Collectively, the data suggests that hospitalized infants, in  
45 combination with their caregivers, shape the microbiome of NICU rooms.

46  
47 **1.2 Keywords**

48  
49 Infant gut, microbiome, built environment, neonatal intensive care unit

50  
51 **1.3 Background**

52 Hospital acquired infections (HAIs) remain a major problem in the US. One out of every  
53 twenty-five patients will experience a HAI, costing the US approximately \$30 billion per year [1].  
54 Infants hospitalized in the neonatal intensive care units (NICU) are particularly susceptible to  
55 infection due to their underdeveloped immune systems [2, 3]. To protect against infection, infants  
56 are often prescribed antibiotics during the first week of life. In fact, antibiotics are three of the six  
57 most commonly administered medications in the NICU [4]. This treatment likely kills microbes  
58 acquired during the birthing process [5] and promotes a categorically different colonization pattern  
59 in preterm infants relative to full term infants [6]. Preterm infants are often colonized by ESKAPE  
60 organisms (*Enterococcus* spp., *Staphylococcus aureus*, *Klebsiella* spp., *Acinetobacter* spp.,  
61 *Pseudomonas aeruginosa*, and other Enterobacteriaceae), which are also the most frequent cause  
62 of nosocomial infections [7]. The relatively sterile preterm infant gut microbiome and the high  
63

frequency at which infants are colonized by hospital associated microbes, creates a valuable study setting to better understand how the room microbiome is shaped by its occupants. Here, we conducted an experiment to quantify and characterize NICU room microbes to enable comparison with microbiomes that develop in the premature infant gut

The source of early stage gut colonizers in preterm infants has been explored to some extent [8–11]. In a pilot study, we tracked two infants over the first month of life, collecting samples from room surfaces and infant fecal samples [12]. Using an amplicon-EMIRGE approach, which allows for recovery of full-length 16S rRNA genes (~1500 b) [13], as opposed to the more common hypervariable region approach (~150-400 b), we detected the same sequences in room samples before they were detected in gut samples. In a much higher resolution genome-resolved metagenomics study we recently showed evidence for the presence of some infant gut associated strains in the NICU room environment and for exchange of those strains between infant and room environments [24].

Recent genomic studies have shown that the vast majority of strains in the premature infant gut are not shared among infants [5]. Nearly 150 strains were recovered from 10 infants' fecal samples and only 4 of these were shared. These samples were collected within a month of each other, suggesting that a multitude of strains are available in the NICU at any given point in time, and only a few strains may be widespread, a conclusion supported by the more recent research [Brooks et al. in revision]. However, a few strains were identified in infant fecal samples collected years apart from different infants housed the same NICU [14]. These were referred to as "persister" strains.

A recent study identified 794 antibiotic resistance genes in preterm infant stool samples, 79% which had not previously been classified as associated with resistance [15]. It is possible that these genes provide a competitive advantage for survival in the highly cleaned room environment [16]. However, in our prior work we found that persister strains, which we infer have a room reservoir, were not found to differ significantly in virulence, antibiotic resistance, or metabolism from non-persister strains.

An important question from the perspective of HAI and microbiome establishment of hospitalized premature infants relates to the diversity and biomass distributions over room environments. To address this knowledge gap, we conducted a study with sixteen infants, whose rooms were sampled Monday through Friday from twenty two room locations. We performed droplet digital PCR (ddPCR) on all room samples to directly quantify biomass (2832 samples in total) to determine how biomass varies in the NICU with additional quantification of negative controls. Overall, the findings provide new information about the NICU microbiome and its relationship to room occupant microbiomes.

## 2 Methods

### 2.1 Sample Collection

Infants were enrolled in the study based on the criteria that they were < 33 weeks gestation and were housed in the same physical location within the NICU during the first month of life. Samples were collected Monday through Friday for days of life (DOL) 5-28. Fecal samples were collected from infant diapers and were stored at -20 °C within 10 minutes of collection for short term storage. Shortly after collection, samples were archived and transferred to a -80 °C freezer

109 for long term storage until DNA extraction. All samples were collected after signed guardian  
110 consent was obtained, as outlined in our protocol to the ethical research board of the University of  
111 Pittsburgh (IRB PRO12100487). This consent included sample collection permissions and consent  
112 to publish study findings.

113 All samples were obtained from a private-style NICU at Magee-Womens Hospital of the  
114 University of Pittsburgh Medical Center. Twenty-two of the most frequently touched surfaces were  
115 determined by visual observation and health care provider interviews in the weeks leading up to  
116 sample collection. Microbial cells were removed from most surfaces using nylon FLOQSwabs  
117 (Copan Diagnostics, Brescia, Italy) and a sampling buffer of 0.15 M NaCl and 0.1% Tween20.  
118 Samples were collected by one research nurse to ensure consistent sampling technique. Ten square  
119 centimeters of each surface was sampled or, for smaller surfaces, the entire surface itself (e.g.,  
120 isolette knobs and sink basin drain grill). Wipe samples were collected from the floor and exterior  
121 top of the isolette using Texwipe TX1086 wipes (Texwipe, Kernersville, NC, USA). Before  
122 collecting each wipe sample, the collector would put on latex examination gloves and clean these  
123 gloves with an isopropanol wipe. The wiped surface area was approximately forty-eight square  
124 centimeters or, for smaller surfaces, the entire surface itself (e.g., isolette top). A wipe was also  
125 used to collect microbial cells at the exterior facet of the heating, ventilation and air conditioning  
126 (HVAC) system. The wipe was suspended via airflow on the exterior (upstream) face of the  
127 MERVE 8 pleated filter, the zone in which supply and return air are mixed before thermal and  
128 humidity treatment of the airstream for four days. Features of the HVAC system are described in  
129 detail in a recently published paper [18].

130 Air samples were collected using the NIOSH two-stage bioaerosol cyclone 251 sampler  
131 [19] and a suspended petri dish method [20]. The NIOSH sampler collected samples continuously  
132 Monday through Friday, comprising approximately 96 hours of sampling at 3.5 L/minute (total  
133 volume sampled = 20 m<sup>3</sup>). Petri dish samples were suspended approximately one meter below the  
134 drop ceiling in the corner of the room that was the furthest away from the sink. These samplers  
135 were maintained in place for the duration of the infant's stay. Petri dish "cooler" samples are plates  
136 that were taped to the top of a cooler which collected abiotic aerosol data [18]. At the end of the  
137 sample collection period, all samples were placed in a sterile transport tube and stored within 10  
138 minutes at -80 °C until further processing.

139

## 140 2.2 DNA extraction and PCR amplification

141

142 DNA was extracted using either the MO BIO PowerSoil DNA Isolation kit (single tube  
143 extractions) or PowerSoil-htp 96 Well DNA Isolation kit (MoBio Laboratories, Carlsbad, CA,  
144 USA). For DNA extracted from feces with the 96-well kit fecal samples were kept frozen on dry  
145 ice and added to individual wells of the bead plate and stored at -80°C until extraction. The day of  
146 extraction Bead Solution and Solution C1 were added and the plates were incubated at 65°C for  
147 10 minutes. The plates were shaken on a Retsch Oscillating Mill MM400 with 96-well plate  
148 adaptors for 10 minutes at speed 20. The plates were rotated 180° and shaken again for 10 minutes  
149 at speed 20. All remaining steps followed the manufacturer's centrifugation protocol. For swab  
150 samples the heads were snapped at the perforation into the wells of the bead plate and stored at -  
151 80°C. The day of extraction the Bead Solution and Solution C1 were added and the plates were  
152 incubated at 65°C for 10 minutes. The plates were shaken on a Retsch Oscillating Mill MM400  
153 with 96 well plate adaptors for 5 minutes at speed 20. The plates were rotated 180° and shaken  
154 again for 5 minutes at speed 20. The Solution C2 and C3 steps were combined (200 µl of each

155 added) to improve DNA yield. All remaining steps followed the manufacturer's centrifugation  
156 protocol.

157 Wipe samples were stored in a sterile 250 mL tissue culture flask upon collection and  
158 thawed on ice before extraction. Cells were dislodged from wipes in a protocol adapted from  
159 Yamamoto *et al.* [17]. Briefly, 150 mL of dislodging buffer was poured into a flask (1X PBS,  
160 0.04% Tween 80, passed through a 0.2  $\mu$ m filter) and the flask was shaken vigorously for one  
161 minute. Supernatant was then decanted into a 250 mL disposable filter funnel with a pore size of  
162 0.2  $\mu$ m (Thermo Scientific, Waltham, MA, USA) and the filter was then placed in a MoBio  
163 PowerWater extraction tube. PowerWater extraction followed manufacturer recommendations.

164 Droplet digital PCR (ddPCR) was adapted from a method previously published on  
165 quantification of 16S rRNA templates in infant fecal samples [5]. The only deviation from the  
166 previous method was that a diluted gDNA template of 1:10 instead of 1:1000 was utilized. Both  
167 MiSeq library preparation and ddPCR were performed in 96-well plate format. Each plate had  
168 three no template PCR controls, one no template extraction control, and three positive controls  
169 containing varying concentrations of purified *E. coli* gDNA. Counts from the negative control  
170 types were averaged across type and the highest was used to correct for contaminant counts in  
171 sample data.

### 173 2.3 Sequencing preparation and sequencing

174 Genomic DNA from room samples were subjected to 16S rRNA V3-4 MiSeq library  
175 preparation which included dual-barcoded multiplexing with a heterogeneity spacer for higher  
176 sequence quality [22]. Two microliters of 5X concentrated gDNA template was used in the  
177 reaction and run at 35 cycles. Amplicons were purified using the Just-a-Plate PCR normalization  
178 and purification kit (Charm Biotech, San Diego, CA, USA). Equal amounts of each sample were  
179 sent to the University of California Davis DNA Technologies Core Facility  
180 (<http://dnatech.genomecenter.ucdavis.edu>) and run on a MiSeq with v3 300PE chemistry.

181 Illumina library construction for infant fecal samples followed standard protocols at  
182 University of California QB3 Vincent J. Coates Genomics Sequencing Core Facility  
183 (<http://qb3.berkeley.edu/gsl/>). Briefly, gDNA was sheared using a Covaris to approximately 600  
184 bp and 1000 bp. Wafergen's PrepX DNA library prep kits were used in conjunction with the  
185 Apollo324 robot following factory recommendations (Integenx). Thirteen cycles of PCR were  
186 used during library construction. Libraries were added at 12 samples per lane, in equimolar  
187 amounts, to the Illumina HiSeq 2500 platform. Paired-end sequences were obtained with 150  
188 cycles and the data processed with Casava version 1.8.2. Raw read data were deposited in the  
189 NCBI Short Read Archive (Bioproject PRJNA376566, SRA SUB2433287).

### 193 2.4 16S amplicon data processing

194 The LotuS 1.562 pipeline in short amplicon mode was used for quality filtering,  
195 demultiplexing, and OTU picking [23]. LotuS was run with the following command line options:  
196 '-refDB SLV,GG -highmem 1 -p miseq -keepUnclassified 1 -simBasedTaxo lambda -threads 10.'  
197 The OTU data was rarefied to 1,000 sequences per sample, without replacement, unless explicitly  
198 stated. OTU table and LotuS log files are available in Additional file 1.

201 **2.5 Metagenomic data from infant gut samples**  
202

203 For comparative purposes, this study made use of previously published infant metagenomic  
204 data from 290 fecal samples collected from infants housed in the NICU rooms studied here (~800  
205 Gb of 150 bp paired-end reads). Methods for data analysis are described within this publication  
206 [24].  
207

208 **3 Results**  
209

210 **3.1 Sequencing summary and contamination removal**  
211

212 In total, 2832 room samples were processed through a MiSeq library preparation protocol.  
213 After quality filtering and demultiplexing, 84,939,529 read pairs were generated. These reads were  
214 clustered into 18,093 OTUs. Using a ratio OTU (ROTU) method that leverages biomass  
215 quantification and sequencing of negative controls [25], 269 OTUs and 925 samples were removed  
216 from the dataset when using an ROTU threshold of 0.001. A second *in silico* contamination  
217 cleaning method was applied [26], which removed an additional 323 OTUs and 1 sample. In total,  
218 approximately 3% of generated OTUs and 33% of samples present too weak of a signal to  
219 confidently distinguish them from negative control signatures.  
220

221 **3.2 Biomass and taxonomic variation across petri dish replicates**  
222

223 Biological and technical replicates performed for petri dish plates established the  
224 reproducibility of extraction of DNA from petri dish swabs and provided evidence for highly  
225 reproducible ddPCR measurements (Additional file 2). The highest standard deviation in ddPCR  
226 values for biological replicates in a single room was 106,760 copies/sample (infant 6's petri plates;  
227 mean = 99,677) and for technical replicates, the largest standard deviation was 15,534  
228 copies/sample (infant 12's petri plates, mean = 81,044). The lowest standard deviation for  
229 biological replicates was 1,981 copies/sample (infant 1's petri plates, mean = 13,785) and 737  
230 copies/sample for technical replicates (infant 11's petri plates, mean = 32,396). Overall, this  
231 equates to a reproducibility range of 2.69 to 6.87 $\times$  more reproducibility across technical ddPCR  
232 runs relative to biological replicates, with an average reproducibility ratio of 5.37 $\times$  better for  
233 technical replicates.  
234

235 **3.3 Biomass varies significantly across sample type**  
236

237 16S rRNA gene copies were quantified for 2,883 samples using ddPCR and showed day-to-  
238 day variation ranging from approximately 4 to 33000 16S rRNA copies/cm<sup>2</sup> (Figure 1a). Samples  
239 from the HVAC system had the highest biomass of all types and bioaerosol samples had the lowest  
240 (Additional file 3 a and b). Sinks had the highest biomass of the swabbed samples and hands had  
241 the lowest average median template count (Figure 1b). Petri dishes suspended from the ceiling had  
242 the lowest biomass relative to other passive dust collectors, whereas the nurse's station dishes  
243 contained the highest bacterial load. The infant room consistently had higher template counts than  
244 the hallway bioaerosol samples. Overall, the median biomass varied over 4 orders of magnitude  
245 across all sample types.

246  
247

248 **3.4 Skin associated taxa dominate the NICU surface environment**

249

250 The microbial communities in most NICU environments were highly uneven and were  
251 dominated by 5-10 OTUs (Figure 2). 41% and 55% of all amplicon reads belong to the top five  
252 and ten OTUs in the NICU, respectively (Figure 2 and Table 1). Most of these taxa are human  
253 associated with many commonly associated with the skin (*Corynebacterium*), mouth  
254 (*Streptococcus*), or nose (*Staphylococcus*). SourceTracker v1.0.1 [27] was run using skin, oral,  
255 and fecal samples from the American Gut project as the putative source database with NICU  
256 samples labeled as “sink” samples. Skin was the most likely contributor to taxa in the NICU,  
257 accounting for upwards of 50% of the most probable sources, followed by oral and fecal samples  
258 (Additional file 4).

259 Samples collected from the HVAC system had the highest bacterial diversity with 405  
260 OTUs on average per sample, whereas bioaerosol samples had the lowest, with 13 (Additional file  
261 5a). The HVAC samples had the highest Shannon community evenness, followed by floor wipes,  
262 and the bioaerosol samples had the lowest Shannon diversity (Additional file 5b). Thus, overall,  
263 the HVAC had highly even consortia with high diversity. This is expected due to the way that the  
264 HVAC sample was collected, with metric tons of air passing through the collection wipe before  
265 sequencing [18]. The NICU room air was also found to have low biomass and low diversity, with  
266 strong dominance by members of the *Aeromonadaceae* in the small size fraction and  
267 *Streptococcaceae*, *Rhizobiaceae*, *Clostridiaceae* in the large size fraction.

268 All touched surfaces had similar numbers of OTUs per sample, although the surface  
269 monitors showed the most unevenness (Additional file 5). These surfaces were dominated by  
270 similar groups of microbes. Although many touched surfaces were associated with skin-associated  
271 bacteria, gut associated Enterobacteriaceae OTUs also dominated environments such as the surface  
272 monitors, counter tops, and scanners (Figure 2). In contrast, the sink basins had comparatively low  
273 numbers of OTUs per sample (Additional file 5a), in part due to the high dominance by four  
274 bacterial groups (Figure 2).

275

276 **3.5 Biomass suggests growth patterns in sink basins**

277

278 A range of 29 to 38 sink basin samples per weekday were collected from 14 unique sink  
279 basins. When comparing biomass trends across days (Figure 3a), a distinct pattern of decreasing  
280 biomass is apparent in sink samples relative to other swabbed environments. In comparing  
281 Shannon diversity across weekdays (Figure 3b), bacterial diversity in Tuesday versus Friday  
282 samples were the most distinct, whereas biomass was most different in Monday versus Thursday  
283 samples (Wilcoxon rank sum, Bonferroni adjusted  $p = 0.47$  and  $0.012$ , respectively). Sink basins  
284 were cleaned approximately every twenty-four hours, but less frequently on the weekends, so the  
285 elevated biomass at the beginning of the week may be due to regrowth of sink adapted taxa  
286 throughout the weekend (e.g., *Rhizobiaceae*, *Pseudomonas*, *Aeromonas*, and *Enterobacteriaceae*).  
287 The increase in Shannon diversity from Monday to Friday strengthens this inference.

288

289 **3.6 NICU rooms harbor a unique microbial signature**

290

291 Using a support vector machine (SVM) classifier with a linear kernel [28], we determined

292 that each room's microbiome contained a unique microbial fingerprint. We could predict the room  
293 origins with an overall accuracy of 56% (when we knew the room's origin but withheld that  
294 information from the classifier), which is 5x better than random chance (Figure 4). The use of  
295 ROTU over a standard pipeline achieved an increase in accuracy of approximately 16%. Typically,  
296 the most confusion occurred between samples that were collected at similar times, although infants  
297 that had similar gut communities had decreased prediction accuracy (e.g. infants 2, 3, and 8).  
298 Important OTUs driving the SVM model are plotted and listed in Additional file 6 and Table 2.  
299 Interestingly, there is an overlap between room specific OTUs that drive the SVM model and  
300 occurrence of these taxa in the gut of infant occupants. For example, the most visible signature in  
301 SVM taxa comes from a spike in *Veillonella* in infant 6's room on DOL 18 (Additional file 6). A  
302 major increase of *Veillonella* in infant 6's gut occurred on DOL 16 (ref  
303 [http://ggkbase.berkeley.edu/project\\_groups/human-gut-metagenome-sloan-infants](http://ggkbase.berkeley.edu/project_groups/human-gut-metagenome-sloan-infants) and Additional  
304 file 7). The same pattern is seen for infant 8, and in fact, most infants that contain *Veillonella* have  
305 strong SVM signals associated with their room. The second strongest signal from the SVM model  
306 comes from a *Clostridium* OTU. This group is present in infants 2, 3, and 8's room samples and it  
307 strongly contributes to the SVM model prediction. All three of these infants have high abundances  
308 of *Clostridium*.  
309

### 310 **3.7 Composition of persister taxa in the room echoes infant gut composition**

311 To visualize the distribution of families with representative strains known to persist in infants  
312 over multi-year periods [14, 15], we collapsed each study day and infant pairing by averaging all  
313 amplicon abundance data across environments (Additional file 8, "average" panel). In this  
314 analysis, the subset of all OTUs that belonged to a persister family was assigned a distinct color  
315 but often one OTU could be distinguished within a family. However, due to high abundance, we  
316 gave OTU\_5 (an *Enterobacteriaceae*) dedicated coloring. Surprisingly, persister families account  
317 for > 50% of the data at many time points.  
318

319 Episodes of particularly high persister family abundance occurred in rooms housing infants  
320 1, 9, 12, and 16. To better visualize which samples contributed to the averaged data (Additional  
321 file 8, "average" panel), we also plotted data for the specific environments for which we had the  
322 most samples (armrests and sinks). Both the armrests and sinks are dominated by these groups of  
323 organisms during these episodes, but *Staphylococcaceae* OTUs are much more abundant in  
324 armrest samples relative to sinks. Two dominant *Pseudomonas* OTUs that comprised 70% and  
325 24% of all *Pseudomonadaceae* (OTU\_8 and OTU\_15, respectively) were detected throughout the  
326 time series, but were at very low abundance in armrest samples over long time spans.  
327

### 328 **Composition of persister taxa in infant 9**

329 Since the room data for infant 9 had a strong signal for persister groups, we analyzed samples  
330 from all environments separately to visualize temporal patterns (Figure 5a). Persister groups  
331 dominated most of infant 9's room samples, with cellphones having the fewest and scanner and  
332 surface counter samples having the most persister groups per sample. The red lines in Figure 5a  
333 highlight the time point where a major increase in relative abundance of *Enterobacteriaceae* taxa  
334 occurred in infant 9's gut (Figure 5b and Additional file 7). This group is present in multiple room  
335 environments prior to the increase, particularly associated with the isolette and armrest. At  
336 subsequent time points, this group becomes highly prominent in some room environments (e.g.,  
337

338 scanner and surface counter).

339 OTUs belonging to the persister groups cannot be confidently classified genus level via 16S  
340 rRNA gene sequencing [29], and since *Enterobacteriaceae* dominates the gut of infant 9, we  
341 leveraged room and fecal sample context to infer a possible identity for OTU\_5. Using OTU\_5's  
342 reference sequence as a query, we ran ublast [30] on a database of 16S rRNA genes reassembled  
343 from infant 9's fecal metagenomic samples using the REAGO algorithm (Yuan *et al.*, 2015). The  
344 top hit to our 429 bp query was 99.5% identical (2 mismatches) and came from several of infant  
345 9's fecal samples. Most of the top hits have the entire 16S rRNA gene recovered from the REAGO  
346 assembly (~1,520 bp). These fecal sequences were searched against the Silva database  
347 (SLV\_119\_SSU) and returned identical, full-length matches to *Klebsiella pneumoniae*. While this  
348 is an extrapolation from the V3-4 region, it is possible that OTU\_5 in the room is a *Klebsiella* and  
349 may be *Klebsiella pneumoniae*, the dominant bacterium colonizing infant 9.

## 350 4 Discussion

351 The first question that we aimed to answer in this study related to how biomass varies across  
352 a NICU. Using ddPCR to quantify 16S rRNA gene copy number, we show biomass density varies  
353 across NICU surfaces by 4-5 orders of magnitude (Figure 1). Surprisingly, the floor in front of the  
354 infant's isolette had the highest density of microbes relative to any other environment within the  
355 NICU. Naively, it may seem intuitive that the region with the most foot traffic, e.g. the floor at the  
356 main entrance of the NICU, would have the highest biomass. While the main entrance floor has a  
357 high density, it is significantly lower than the floor in front of the isolette. This finding may be due  
358 to the increased occupancy at the isolette versus the main entrance, where occupancy is more  
359 transient.

360 Petri dish data also suggest that higher levels of human activity drive higher amounts of  
361 microbial deposition in the room environment. The nursing station has higher petri dish-associated  
362 biomass than the infant room, followed by the hallway (Figure 1). This outcome occurred despite  
363 the fact that the infant room and hallway coolers collected dust at the same height (1 m), whereas  
364 the nurse station collector was at approximately double the height (1.8 m). As height above the  
365 floor increases, detection of resuspended particles from dust decreases exponentially [32, 33]. This  
366 finding suggests that floor dust is not the main source of biological particles accumulated in the  
367 petri dishes, but rather the microbes are human-derived. Greater occupancy or rigor of activity  
368 [34] at the nursing station compared to the infant room and hallway likely explains this result.

369 A recently published study noted a stronger occupancy signal from the occupancy sensors in  
370 the infant room compared to the hallway [18]. The occupancy signal directly overlapped with the  
371 coarse particle signal (which detected particles > 10  $\mu\text{m}$  in diameter). This signal was interpreted  
372 to indicate that resuspension or deposition of particles from occupants is the largest contributor of  
373 aerosolized particles in the NICU. In the current study, our Petri dish ceiling analyses suggest a  
374 similar conclusion for settled particles, but in this case based on biological data.

375 If occupancy is a key feature of the NICU environment, one would expect human associated  
376 microbes to dominate in most room environments. We found that 5-10 OTUs account for most of  
377 the amplicon data and a majority of these are typically skin, nose, or fecal associated (Figure 2).  
378 The enrichment of human associated taxa is likely due to tight control of the building envelope via  
379 HVAC treatment [35] combined with a strict cleaning schedule.

380 An interesting finding of this study related to the change in biomass and microbial  
381 community structure of the sink basins over the course of the week. We attribute this pattern to  
382 the room cleaning regime, which is more limited on weekend days than during the week. On

384 Mondays, the sink biomass is highest (Figure 3a) and communities are relatively uneven (Figure  
385 3b), presumably due to extensive growth of a few sink-associated taxa over the weekend. More  
386 intensive cleaning of the sink early in the week likely removes the majority of biomass, which is  
387 comprised of the sink-adapted taxa and enables detection of a wider diversity of low abundance,  
388 poorly adapted or transient, taxa.

389 The second question addressed in our study related to the taxa that dominate NICU surfaces.  
390 To investigate this, it was necessary to adapt a method to eliminate spurious contaminant-based  
391 signals in data from low biomass samples [25]. The ROTU cleaning method implemented here to  
392 clean data of spurious OTUs and contaminants *in silico* was made possible due to the availability  
393 of ddPCR quantification of negative controls. This capability is particularly important for NICU  
394 studies since the rooms are cleaned regularly, causing low biomass levels to be present in many  
395 samples. Some of the bacteria that we conclude were introduced in sample processing are skin  
396 associated, although many types of taxa were encountered. After accounting for contamination,  
397 we conclude that human associated taxa dominate most surfaces.

398 Human associated taxa are likely sourced and trafficked throughout the NICU by healthcare  
399 providers [36] and many hand hygiene studies have reported as much [37]. Here, we implemented  
400 a machine learning classifier to address the possibility that infants and their caretakers shape the  
401 microbiome to be distinctive in each room. Our model reliably classified samples of unknown  
402 origin to their correct room-infant pair at an accuracy two times better than a recently published  
403 office microbiome study [28] and achieved predictive power five times better than random chance.  
404 This outcome suggests that NICU rooms are more personalized than other common built  
405 environments. There are typically a larger variety of activities and people in office spaces and air  
406 treatment is less (lower air exchange rates and less filtration). The combination of less frequent  
407 cleaning, increased occupancy, and more unfiltered outdoor air supply drives many of the  
408 differences between other common indoor environments and the NICU. The more unique room  
409 signal based on NICU room microbes suggests a localized source of bacteria, since a more diffuse  
410 source would lower prediction accuracy. A similar result was recently described in a microbiome  
411 study conducted in a Chicago hospital [38]. Microbial community similarity increased between  
412 patients' hand and floor samples over time, highlighting the exchange between patient and room.  
413 Interestingly, infants in this cohort are rarely removed from their isolettes, so room specific  
414 microbiomes were likely mediated by health care providers, rather than direct infant interaction  
415 with surrounding room surfaces.

416 Finally, we tested for patterns of association between room occupants and NICU room  
417 environments. We found that many taxa driving our machine learning model for the room  
418 microbiome were from groups also present in the gut of the infant occupant. Other signals came  
419 from *Firmicutes* and *Actinobacteria* not affiliated with the infant gut and that were relatively  
420 uniquely detected in certain rooms. Focusing on the subset of taxa that are gut colonizers, we show  
421 a relatively high abundance of these taxa throughout the sampling campaign (Additional file 8).  
422 Episodes where persistent families increase and 2-3 OTUs comprise > 30% of the data across all  
423 environments occurred several times throughout the study (e.g., in infants 9, 12, and 16). These  
424 OTUs are detected in low abundance in the room before detection in the gut (Figure 5). Once in  
425 the infant gut, a far more favorable environment for growth and reproduction than on exposed  
426 hospital surfaces, bacterial density can reach nearly 10 billion cells per gram [5]. After a spike in  
427 relative abundance in the gut, we see these organisms increase in abundance in the room  
428 environment. It is impossible to resolve room 16S rRNA amplicon data to the strain-level in order  
429 to make claims that the same gut bloom resulted in a subsequent expanded appearance in the room.

430 Potentially, infant 9's dominant gut *Klebsiella pneumonia* may be linked to an increased  
431 abundance of Enterobacteriaceae in the room. Interestingly, the same strain of *K. pneumoniae*  
432 found in the gut was detected years apart in different infants within this NICU [14].  
433

434 **5 Conclusions**

435

436 Based on the current study, we conclude that two factors shape room microbiomes. First,  
437 our taxa identifications and occupancy results extend prior findings of a strong link between human  
438 activity levels and room microbiology [12, 18, 24, 34] In fact, this connection appears to be strong  
439 enough to give rise to a relatively unique room microbiome character. Second, environmental  
440 stresses, likely associated with cleaning [12, 16, 39–41], likely selectively shape NICU  
441 microbiomes, primarily by selecting for microbial specialists that can both thrive in the gut and  
442 tolerate the NICU environment. While daily cleaning substantially lowers the bioburden in the  
443 NICU [42], the harshest cleaning methods cannot sterilize hospital surfaces [7]. Creative new  
444 approaches to displace or prevent entrenchment of these NICU specialists, possibly through  
445 prebiotic building materials or clever probiotics, may present opportunities to break the room-  
446 occupant cycle.  
447

448 **6 Declarations**

449

450

451 **7 Ethics approval and consent to participate**

452

453 All samples were collected after signed guardian consent was obtained, as outlined in our  
454 protocol to the ethical research board of the University of Pittsburgh (IRB PRO12100487). This  
455 consent included sample collection permissions and consent to publish study findings.  
456

457 **8 Consent for publication**

458

459 Consent was obtained to publish study findings (IRB PRO12100487).  
460

461 **9 Availability of data and materials**

462

463 Raw read data were deposited in the NCBI Short Read Archive (Bioproject PRJNA376566, SRA  
464 SUB2433287). OTU table and LotuS log files are available at <https://goo.gl/zQf7FY>.  
465

466 **10 Competing Interests**

467

468 The authors declare that they have no competing interests.  
469

470 **11 Funding**

471

472 Funding was provided through the Alfred P. Sloan Foundation under grant APSF-2012-10-05, NIH under grant 5R01AI092531 and the National Science Foundation's Graduate Research Fellowship Program to BB and MRO. This work used the Vincent J. Coates Genomics Sequencing Laboratory at UC Berkeley, supported by NIH S10 OD018174 Instrumentation Grant.

473

474

475

476

477 **12 Authors' Contributions**

478

479 JFB, MJM, and BB conceived of the project. RB organized cohort recruitment and sample

480 collections. BAF conducted nucleic acid extractions. BB, DG, SRR, KRS, and DD conducted

481 ddPCR quantifications and MiSeq library preparations. BB conducted the metagenomic

482 assemblies, BCT provided bioinformatics support and MRO contributed to data analysis. BB and

483 JFB wrote the final manuscript. All authors have read and approved the manuscript.

484

485 **13 Acknowledgments**

486

487 **14 References**

488

489 **1. Healthcare-associated Infections**

490 [<http://www.cdc.gov/winnablebattles/healthcareassociatedinfections/>]

491 2. Arrieta M-C, Stiemsma LT, Dimitriu PA, Thorson L, Russell S, Yurist-Doutsch S, Kuzeljevic  
492 B, Gold MJ, Britton HM, Lefebvre DL, Subbarao P, Mandhane P, Becker A, McNagny KM,  
493 Sears MR, Kollmann T, Mohn WW, Turvey SE, Brett Finlay B: **Early infancy microbial and**  
494 **metabolic alterations affect risk of childhood asthma.** *Sci Transl Med* 2015, **7**:307ra152.

495 3. Cahenzli J, Köller Y, Wyss M, Geuking MB, McCoy KD: **Intestinal microbial diversity**  
496 **during early-life colonization shapes long-term IgE levels.** *Cell Host Microbe* 2013, **14**:559–  
497 570.

498 4. Gasparrini AJ, Crofts TS, Gibson MK, Tarr PI, Warner BB, Dantas G: **Antibiotic**  
499 **perturbation of the preterm infant gut microbiome and resistome.** *Gut Microbes* 2016,  
500 7:443–9.

501 5. Raveh-Sadka T, Thomas BC, Singh A, Firek B, Brooks B, Castelle CJ, Sharon I, Baker R,  
502 Good M, Morowitz MJ, Banfield JF: **Gut bacteria are rarely shared by co-hospitalized**  
503 **premature infants, regardless of necrotizing enterocolitis development.** *Elife* 2015, **2015**:1–  
504 25.

505 6. Groer MW, Luciano AA, Dishaw LJ, Ashmeade TL, Miller E, Gilbert JA: **Development of**  
506 **the preterm infant gut microbiome: a research priority.** *Microbiome* 2014, **2**:38.

507 7. Hu H, Johani K, Gosbell IB, Jacombs ASW, Almatroudi A, Whiteley GS, Deva AK, Jensen S,  
508 Vickery K: **Intensive care unit environmental surfaces are contaminated by multidrug-**  
509 **resistant bacteria in biofilms: Combined results of conventional culture, pyrosequencing,**  
510 **scanning electron microscopy, and confocal laser microscopy.** *J Hosp Infect* 2015, **91**:35–44.

511 8. Shin H, Pei Z, Martinez KA, Rivera-Vinas JI, Mendez K, Cavallin H, Dominguez-Bello MG:  
512 **The first microbial environment of infants born by C-section: the operating room**  
513 **microbes.** *Microbiome* 2015, **3**:59.

514 9. Bäckhed F, Roswall J, Peng Y, Feng Q, Jia H, Kovatcheva-Datchary P, Li Y, Xia Y, Xie H,  
515 Zhong H, Khan MT, Zhang J, Li J, Xiao L, Al-Aama J, Zhang D, Lee YS, Kotowska D, Colding  
516 C, Tremaroli V, Yin Y, Bergman S, Xu X, Madsen L, Kristiansen K, Dahlgren J, Jun W:  
517 **Dynamics and stabilization of the human gut microbiome during the first year of life.** *Cell*  
518 *Host Microbe* 2015, **17**:690–703.

519 10. Chu DM, Ma J, Prince AL, Antony KM, Seferovic MD, Aagaard KM: **Maturation of the**  
520 **infant microbiome community structure and function across multiple body sites and in**  
521 **relation to mode of delivery.** *Nat Publ Gr* 2017(August 2016).

522 11. Dominguez-Bello MG, Costello EK, Contreras M, Magris M, Hidalgo G, Fierer N, Knight R:  
523 **Delivery mode shapes the acquisition and structure of the initial microbiota across multiple**  
524 **body habitats in newborns.** *Proc Natl Acad Sci U S A* 2010, **107**:11971–5.

525 12. Brooks B, Firek BBA, Miller CCS, Sharon I, Thomas BC, Baker R, Morowitz MJ, Banfield  
526 JF: **Microbes in the neonatal intensive care unit resemble those found in the gut of**  
527 **premature infants.** *Microbiome* 2014, **2**:1.

528 13. Miller CS, Baker BJ, Thomas BC, Singer SW, Banfield JF: **EMIRGE: reconstruction of**  
529 **full-length ribosomal genes from microbial community short read sequencing data.** *Genome*  
530 *Biol* 2011, **12**:R44.

531 14. Raveh-Sadka T, Firek B, Sharon I, Baker R, Brown CT, Thomas BC, Morowitz MJ, Banfield  
532 JF: **Evidence for persistent and shared bacterial strains against a background of largely**  
533 **unique gut colonization in hospitalized premature infants.** *ISME J* 2016, **10**:2817–2830.

534 15. Gibson MK, Wang B, Ahmadi S, Burnham C-AD, Tarr PI, Warner BB, Dantas G:  
535 **Developmental dynamics of the preterm infant gut microbiota and antibiotic resistome.** *Nat*  
536 *Microbiol* 2016, **1**:16024.

537 16. Buffet-Bataillon S, Branger B, Cormier M, Bonnaure-Mallet M, Jolivet-Gougeon A: **Effect**  
538 **of higher minimum inhibitory concentrations of quaternary ammonium compounds in**  
539 **clinical *E. coli* isolates on antibiotic susceptibilities and clinical outcomes.** *J Hosp Infect*  
540 2011, **79**:141–6.

541 17. **Strain-resolved community genomic analysis of gut microbial colonization in a**  
542 **premature infant Michael J. Morowitz.** 2010.

543 18. Licina D, Bhagat S, Brooks B, Baker R, Firek B, Tang X, Morowitz MJ, Banfield JF,  
544 Nazaroff WW, Berkeley UC, Jillian F, William W: **Concentrations and sources of airborne**  
545 **particles in a neonatal intensive care unit.** *PLoS One* 2016, **11**:e0154991.

546 19. Lindsley WG, Blachere FM, Thewlis RE, Vishnu A, Davis KA, Cao G, Palmer JE, Clark  
547 KE, Fisher MA, Khakoo R, Beezhold DH: **Measurements of airborne influenza virus in**  
548 **aerosol particles from human coughs.** *PLoS One* 2010, **5**:e15100.

549 20. Adams RI, Miletto M, Taylor JW, Bruns TD: **Dispersal in microbes: fungi in indoor air**  
550 **are dominated by outdoor air and show dispersal limitation at short distances.** *ISME J*  
551 2013, **7**:1262–73.

552 21. Yamamoto N, Shendell DG, Peccia J: **Assessing allergenic fungi in house dust by floor**  
553 **wipe sampling and quantitative PCR.** *Indoor Air* 2011, **21**:521–30.

554 22. Fadrosh DW, Ma B, Gajer P, Sengamalay N, Ott S, Brotman RM, Ravel J: **An improved**  
555 **dual-indexing approach for multiplexed 16S rRNA gene sequencing on the Illumina MiSeq**  
556 **platform.** *Microbiome* 2014, **2**:6.

557 23. Hildebrand F, Tadeo R, Voigt AY, Bork P, Raes J: **LotuS: an efficient and user-friendly**  
558 **OTU processing pipeline.** *Microbiome* 2014, **2**:1–7.

559 24. Brooks B, Olm MR, Firek BA, Baker R, Thomas BC, Morowitz MJ, Banfield JF: **Strain-**

560 **resolved analysis of hospital rooms and infants reveals overlap between the human and**  
561 **room microbiome.** *Nat Commun* 2017, **In Review.**

562 25. Lazarevic V, Gaia N, Girard M, Schrenzel J: **Decontamination of 16S rRNA gene**  
563 **amplicon sequence datasets based on bacterial load assessment by qPCR.** *BMC Microbiol*  
564 2016, **16**:73.

565 26. Meadow JF, Altrichter AE, Bateman AC, Stenson J, Brown G, Green JL, Bohannan BJM:  
566 **Humans differ in their personal microbial cloud.** *PeerJ* 2015, **3**:e1258.

567 27. Knights D, Kuczynski J, Charlson E, Zaneveld J, Mozer MC, Collman RG, Bushman FD,  
568 Knight R, Kelley ST: **Bayesian community-wide culture-independent microbial source**  
569 **tracking.** *Nat Methods* 2011, **8**:761–3.

570 28. Chase J, Fouquier J, Zare M, Sonderegger DL, Knight R, Kelley ST, Siegel J, Caporaso JG:  
571 **Geography and location are the primary drivers of office microbiome composition.**  
572 *mSystems* 2016, **1**:e00022-16.

573 29. Jovel J, Patterson J, Wang W, Hotte N, O'Keefe S, Mitchel T, Perry T, Kao D, Mason AL,  
574 Madsen KL, Wong GKS: **Characterization of the gut microbiome using 16S or shotgun**  
575 **metagenomics.** *Front Microbiol* 2016, **7**(APR):1–17.

576 30. Edgar RC: **Search and clustering orders of magnitude faster than BLAST.**  
577 *Bioinformatics* 2010, **26**:2460–1.

578 31. Yuan C, Lei J, Cole J, Sun Y: **Reconstructing 16S rRNA genes in metagenomic data.**  
579 *Bioinformatics* 2015, **31**:i35–i43.

580 32. Luoma M, Batterman SA: **Characterization of particulate emissions from occupant**  
581 **activities in offices.** *Indoor Air* 2001, **11**:35–48.

582 33. Fairchild CI, Tillery MI: **Wind tunnel measurements of the resuspension of ideal**  
583 **particles.** *Atmos Environ* 1982, **16**:229–38.

584 34. Bhangar S, Brooks B, Firek B, Licina D, Tang X, Morowitz MJ, Banfield JF, Nazaroff WW:  
585 **Pilot study of sources and concentrations of size-resolved airborne particles in a neonatal**  
586 **intensive care unit.** *Build Environ* 2016, **106**:10–19.

587 35. Kembel SW, Jones E, Kline J, Northcutt D, Stenson J, Womack AM, Bohannan BJ, Brown  
588 GZ, Green JL: **Architectural design influences the diversity and structure of the built**  
589 **environment microbiome.** *ISME J* 2012, **6**:1469–79.

590 36. Kembel SW, Meadow JF, O'Connor TK, Mhuireach G, Northcutt D, Kline J, Moriyama M,  
591 Brown GZ, Bohannan BJM, Green JL: **Architectural design drives the biogeography of**  
592 **indoor bacterial communities.** *PLoS One* 2014, **9**:e87093.

593 37. Luangasanatip N, Hongsuwan M, Limmathurotsakul D, Lubell Y, Lee AS, Harbarth S, Day  
594 NPJ, Graves N, Cooper BS: **Comparative efficacy of interventions to promote hand hygiene**  
595 **in hospital: systematic review and network meta-analysis.** *BMJ* 2015, **351**:h3728.

596 38. Lax S, Sangwan N, Smith D, Larsen P, Handley KM, Richardson M, Guyton K, Krezalek M,  
597 Shogan BD, Defazio J, Flemming I, Shakhsheer B, Weber S, Landon E, Garcia-Houchins S,  
598 Siegel J, Alverdy J, Knight R, Stephens B, Gilbert JA: **Bacterial colonization and succession in**  
599 **a newly opened hospital.** *Sci Transl Med* 2017, **9**:1–11.

600 39. Romanova NA, Gawande P V, Brovko LY, Griffiths MW: **Rapid methods to assess**  
601 **sanitizing efficacy of benzalkonium chloride to *Listeria monocytogenes* biofilms.** *J Microbiol*  
602 *Methods* 2007, **71**:231–7.

603 40. Weiss-Muszkat M, Shakh D, Zhou Y, Pinto R, Belausov E, Chapman MR, Sela S: **Biofilm**  
604 **formation by and multicellular behavior of *Escherichia coli* O55:H7, an atypical**  
605 **enteropathogenic strain.** *Appl Environ Microbiol* 2010, **76**:1545–54.

606 41. Hoffman LR, D'Argenio DA, MacCoss MJ, Zhang Z, Jones RA, Miller SI: **Aminoglycoside**  
607 **antibiotics induce bacterial biofilm formation.** *Nature* 2005, **436**:1171–5.

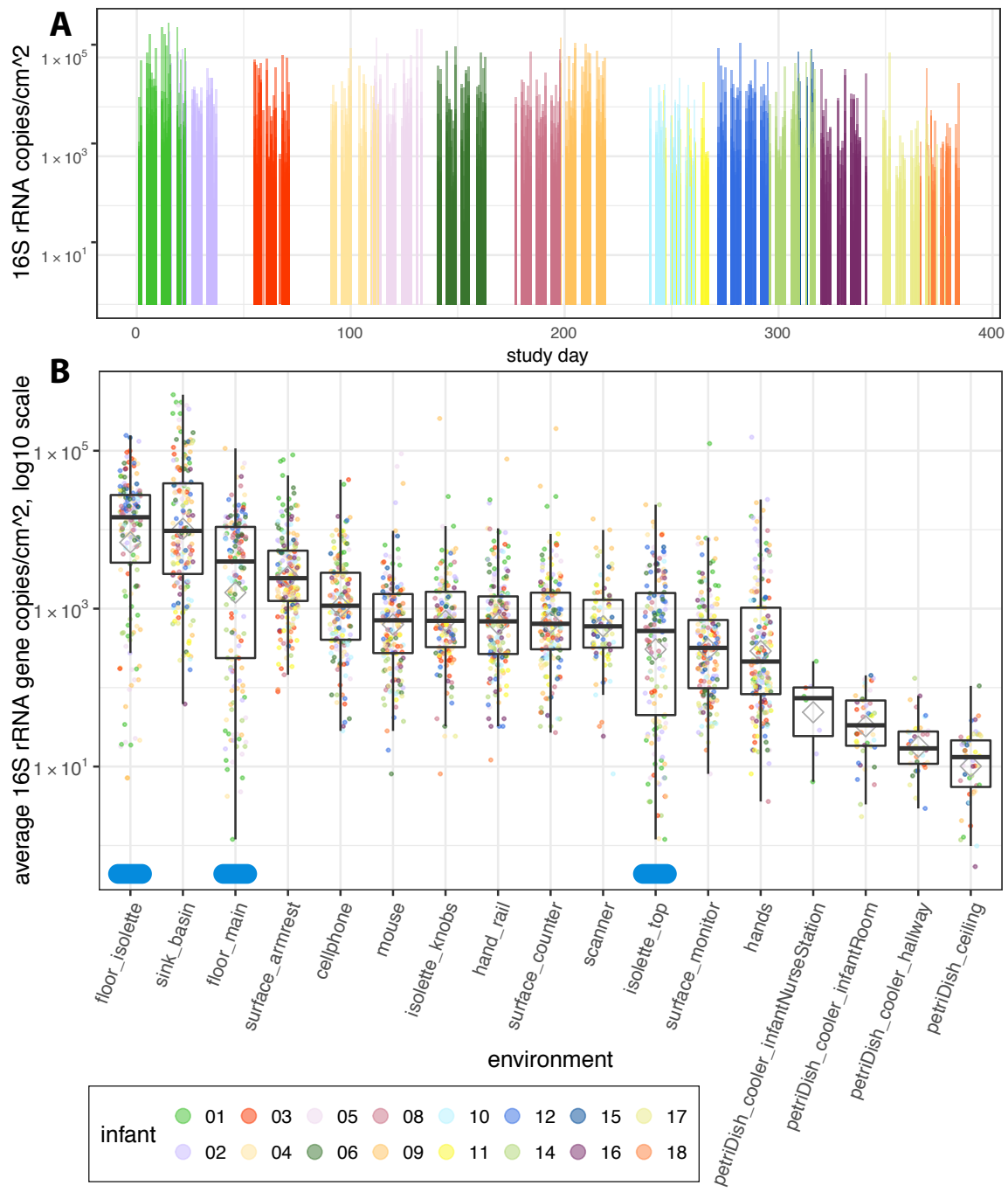
608 42. Bokulich NA, Mills DA, Underwood M a.: **Surface microbes in the neonatal intensive**  
609 **care unit: Changes with routine cleaning and over time.** *J Clin Microbiol* 2013, **51**:2617–24.

610

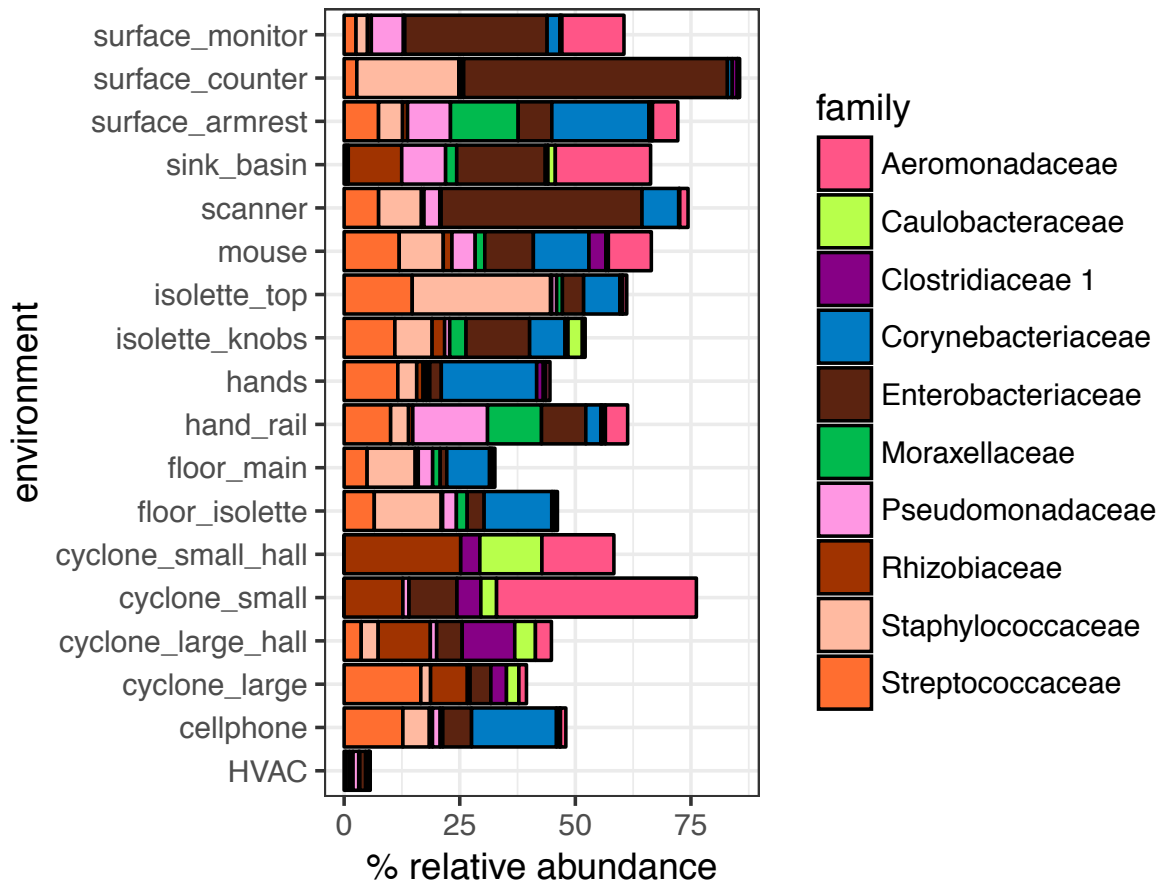
611

## 612 15 Figure legends

Figure 1: **Biomass varies by 4-5 orders of magnitude in a NICU.** 16S rRNA template copy number was quantified via ddPCR. (A) Biomass was averaged across all swab and wipe samples for each sampling day and plotted on a timeline to visualize variation in biomass over the sampling campaign. (B) Each dot reflects the average across triplicate runs. Grey diamonds represent averages per environment. Blue ellipses along the x-axis represent samples collected using a wipe method. All other samples were collected with swabs or using a petri plate to collect settled dust (noted in label). All counts are normalized to represent one day of collection.

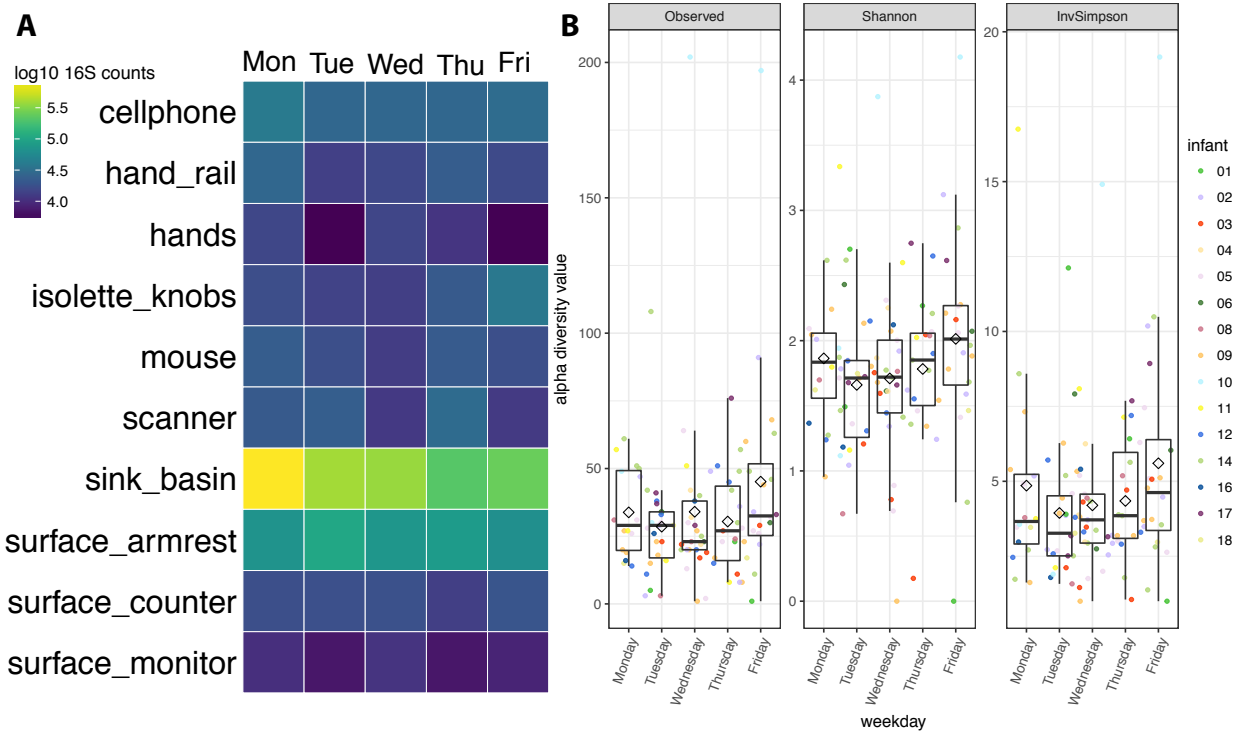


622 Figure 2: **Top 10 NICU OTUs comprise > 50% of NICU taxa.** Amplicon data from a 16S  
623 rRNA V3-4 workflow is plotted for each environment. Only the top 10 OTUs, determined from  
624 averages across all samples, are plotted. Each OTU is colored by its family-level classification.



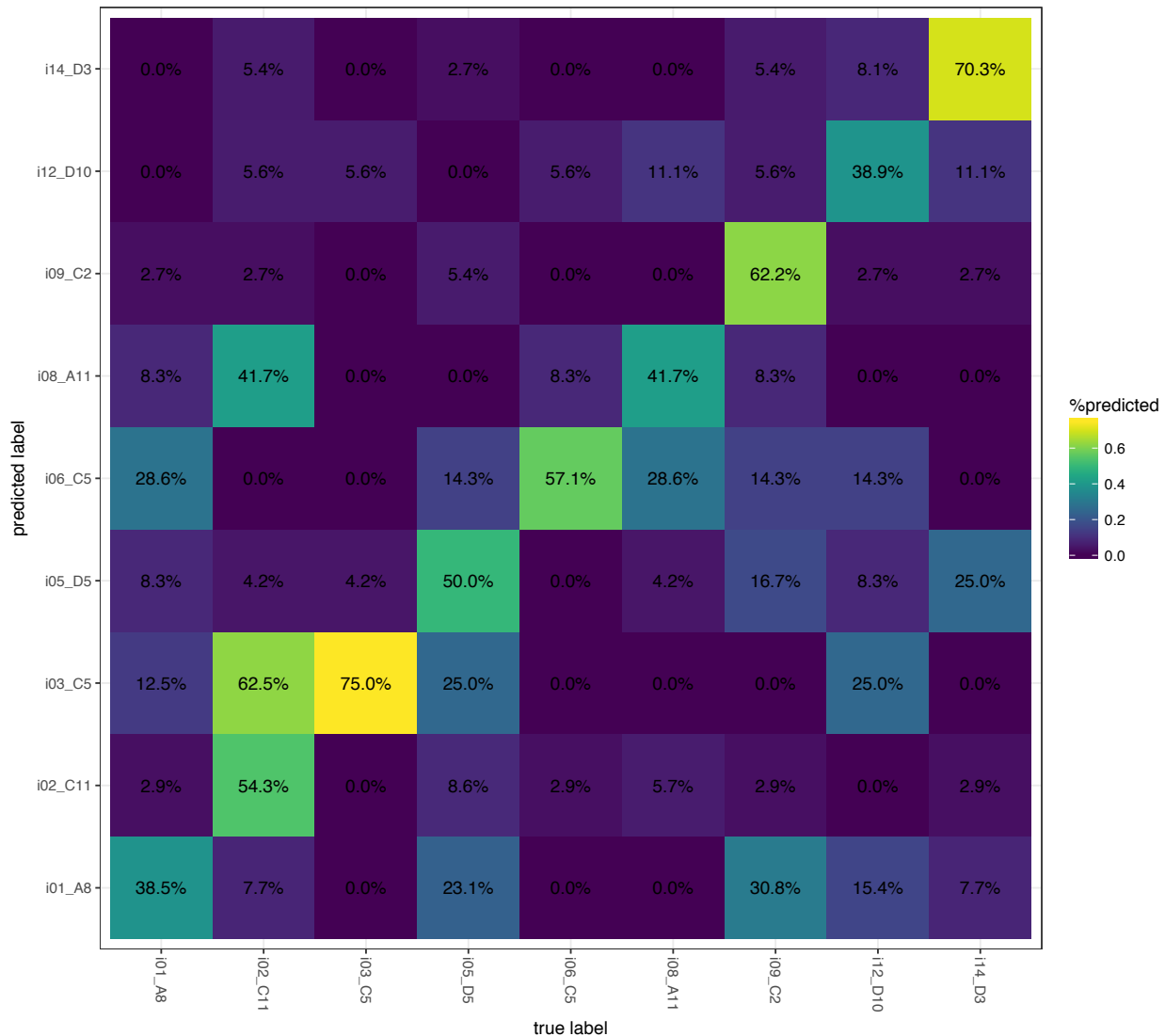
625  
626  
627

628 Figure 3: **Growth detected in NICU sink samples.** 16S rRNA template copy number was  
 629 quantified via ddPCR. Average copy number was averaged for each weekday and swabbed  
 630 environment and displayed in this heatmap (a). 16S rRNA amplicon data was used to calculate  
 631 number of OTUs, Shannon, and Inverse Simpson diversity metrics for sink basin samples (b).  
 632 Black diamonds represent averages per weekday.



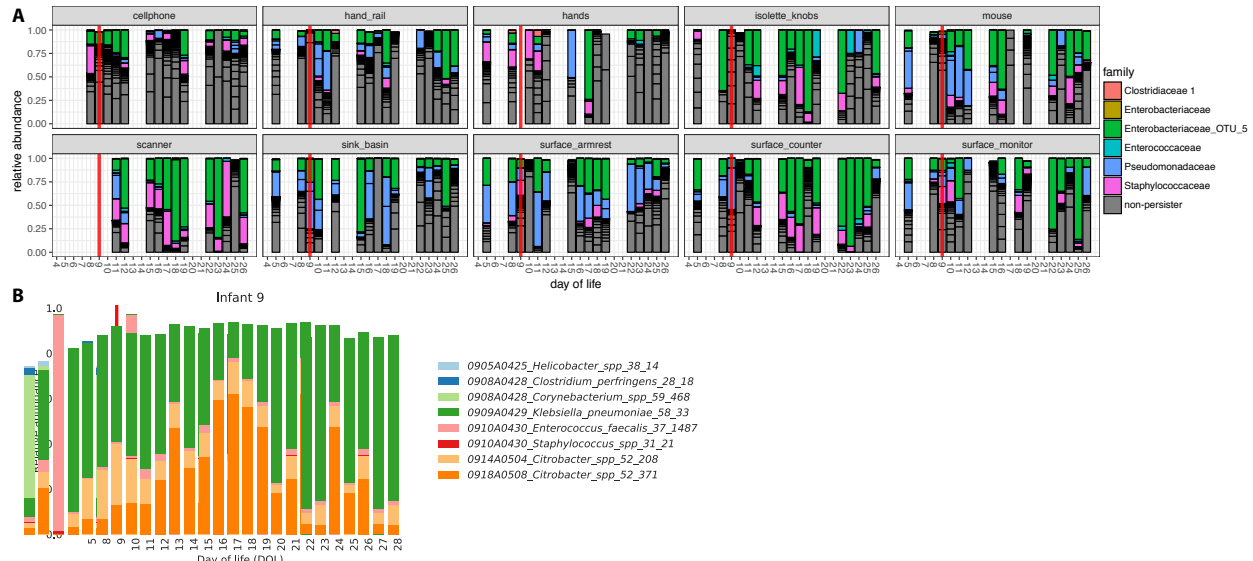
633  
 634  
 635

636 Figure 4: **NICU rooms have a unique microbial signature.** 16S rRNA amplicon data was split  
 637 into training, test, and validation sets to train, test, and validate a support vector machine classifier.  
 638 The confusion matrix plots the accuracy of our model on the validation dataset. Percentages note  
 639 the number of times a sample was predicted to belong to a room-infant pairing divided the total  
 640 number of samples for that room-infant pairing. The heat coloring is based on shown percentages.



641  
 642  
 643

644 Figure 5: **'Persister taxa in the room reflect composition of the infant gut.** Infant 9's room  
 645 amplicons are plotted for each swabbed environment (a). Colored are OTUs that belong to a  
 646 persister lineage. Red lines highlight day of life 9, which coincides with an increase of several  
 647 *Enterobacteriaceae* taxa in the infant gut (b). (b) is the microbial profile for fecal samples  
 648 generated via genomes recovered from a metagenomics approach.



649  
 650  
 651  
 652  
 653  
 654

655 **16 Additional file legends**

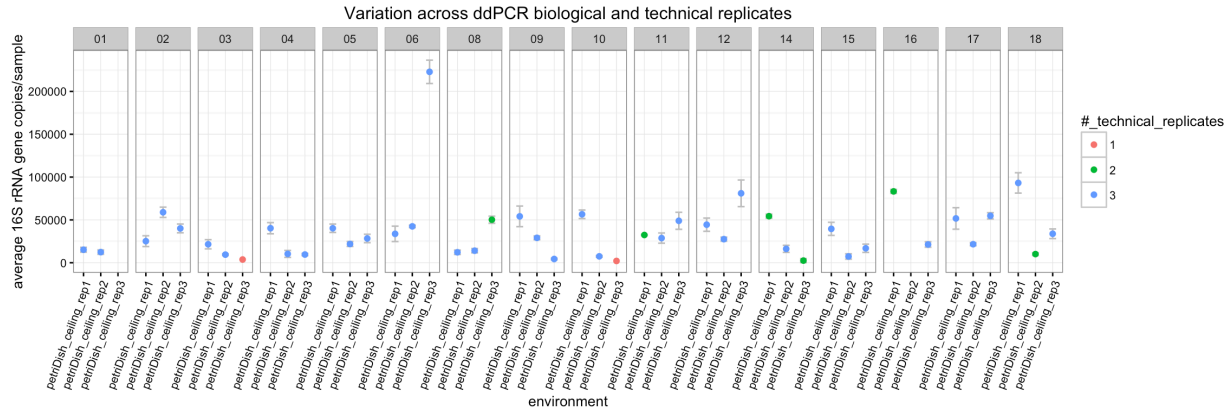
656

657 Additional file 1: **OTU table and LotuS log files**. Output from the LotuS pipeline is provided  
658 including raw OTU table, accompanying mapping file with cohort and ddPCR count data, and  
659 accompanying log files.

660

661

662 Additional file 2: **Biological and technical variation across ddPCR replicates.** 16S rRNA  
 663 template copy number was quantified via ddPCR for three petri dish dust collectors suspended  
 664 from the drop ceiling in each infant's room. Each dot reflects the average across triplicates runs.  
 665 Each infant set is labeled at the top of the plot facets.

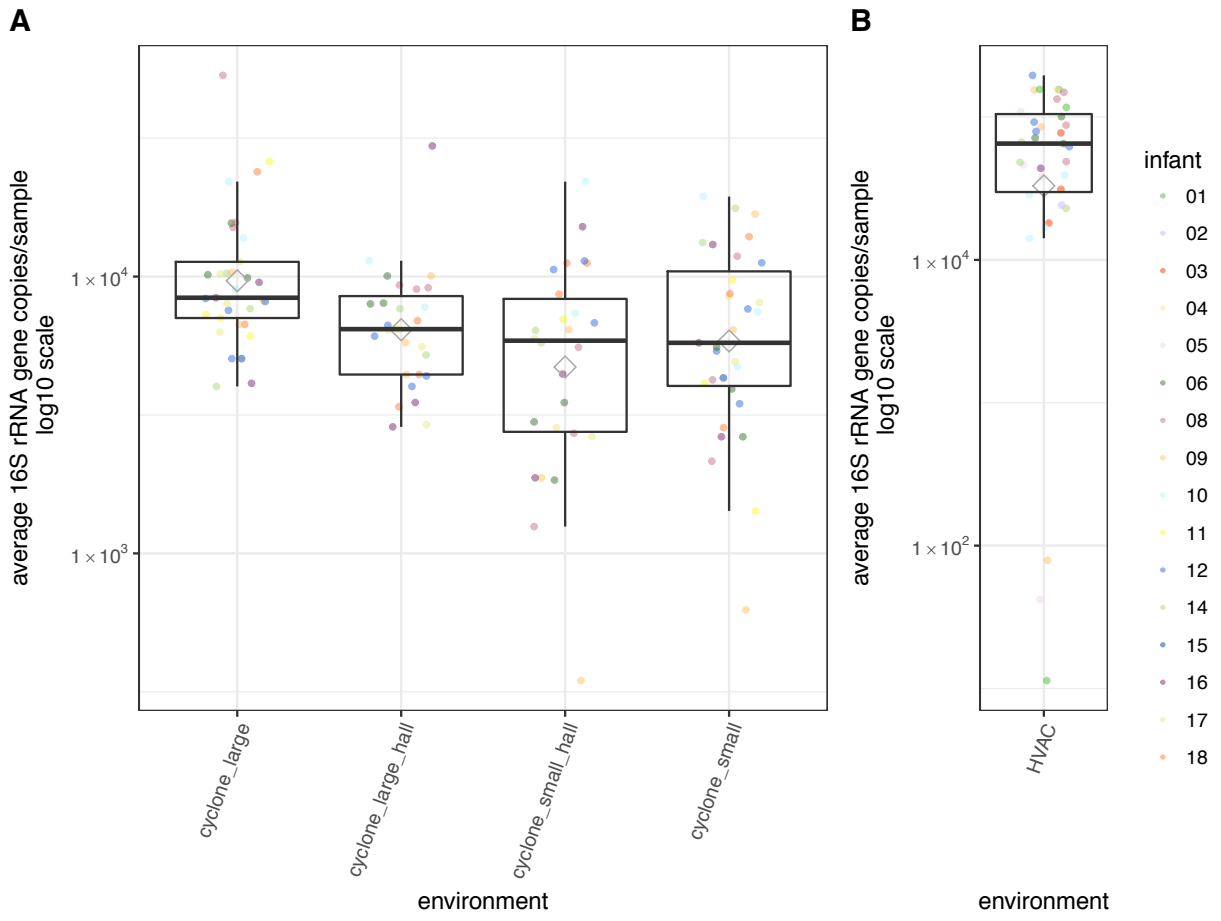


666

667

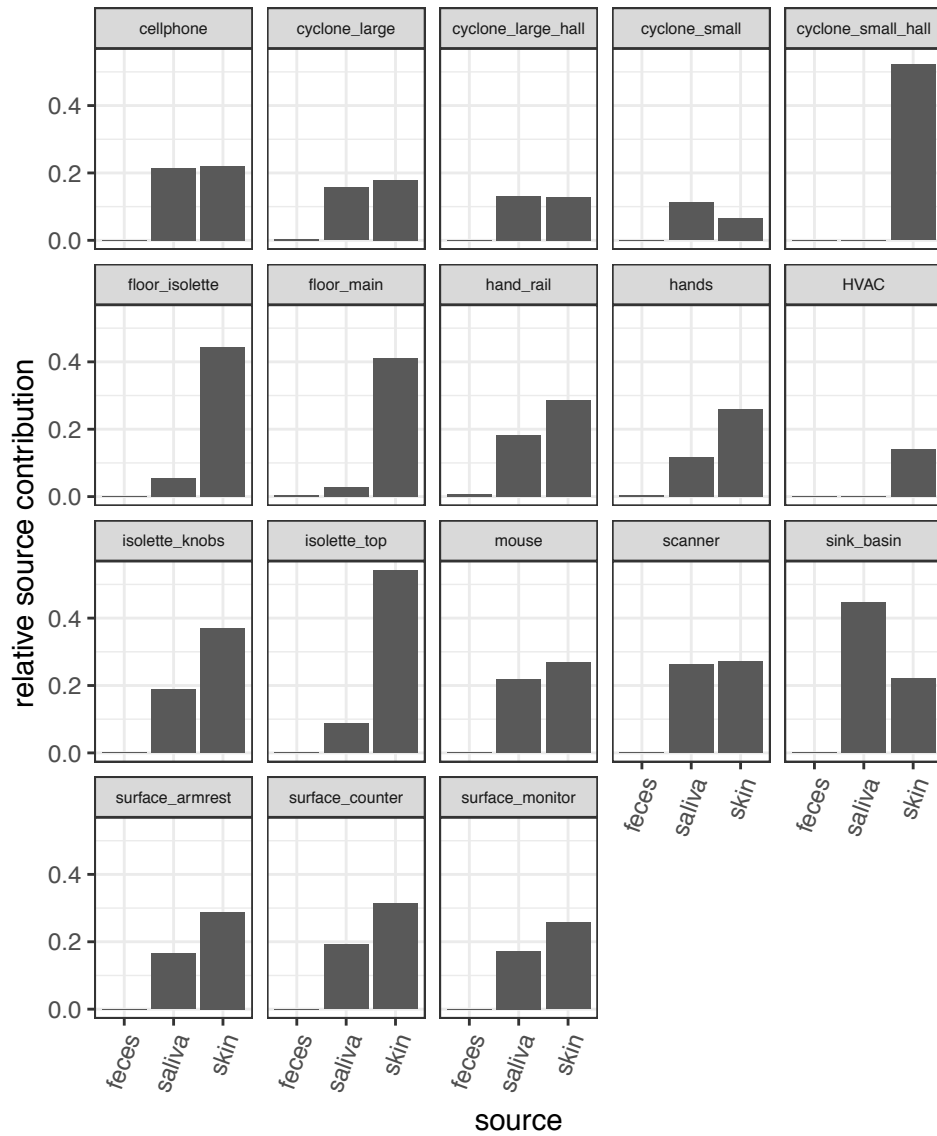
668

669 Additional file 3: **Biomass in air samples from a NICU.** 16S rRNA template copy number was  
 670 quantified via ddPCR. Each dot reflects the average across triplicates runs. Grey diamonds  
 671 represent averages per environment. Bioaerosol measurements in (A) are separated by small and  
 672 large size fractions (particles 1-4  $\mu\text{m}$  and  $> 4 \mu\text{m}$ , respectively). HVAC samples in (B) were  
 673 collected from the exterior facet of the HVAC system and represent pretreated air. Counts are  
 674 normalized per sample per day of collection.



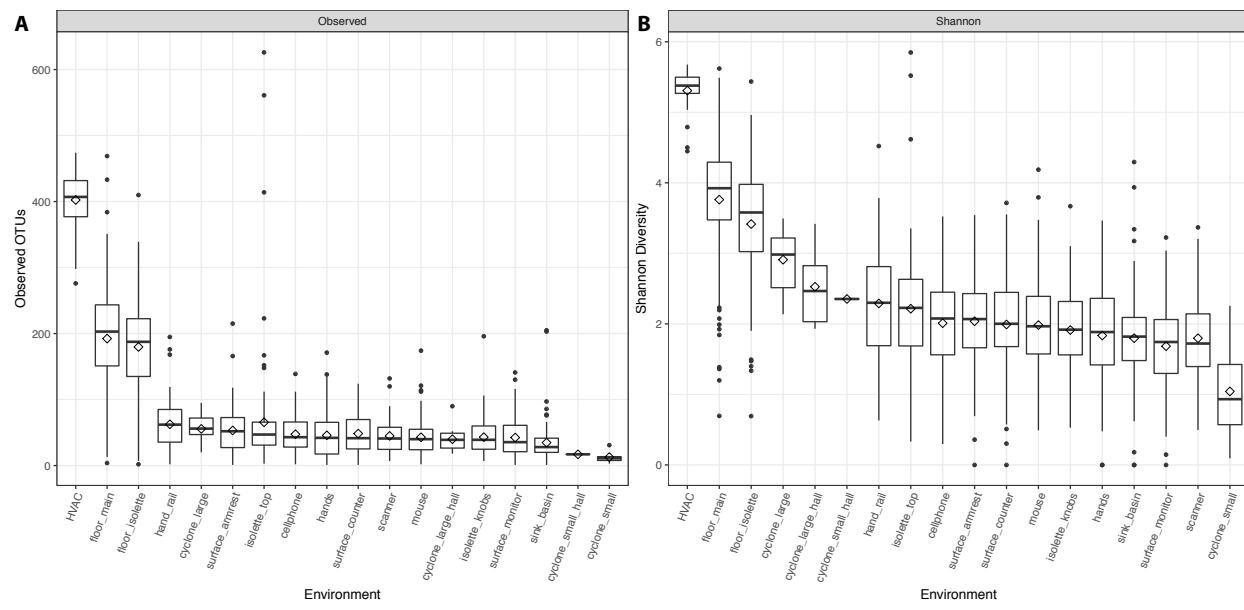
675  
676  
677

678 Additional file 4: **SourceTracker reveals human skin is dominant source of NICU microbes.**  
 679 American Gut skin, oral, and fecal samples were used as “sources” and NICU room samples  
 680 were used as “sinks” and input into the SourceTracker software. Plotted on the y-axis is the mean  
 681 relative contribution of each human-associated source to each environmental sample.



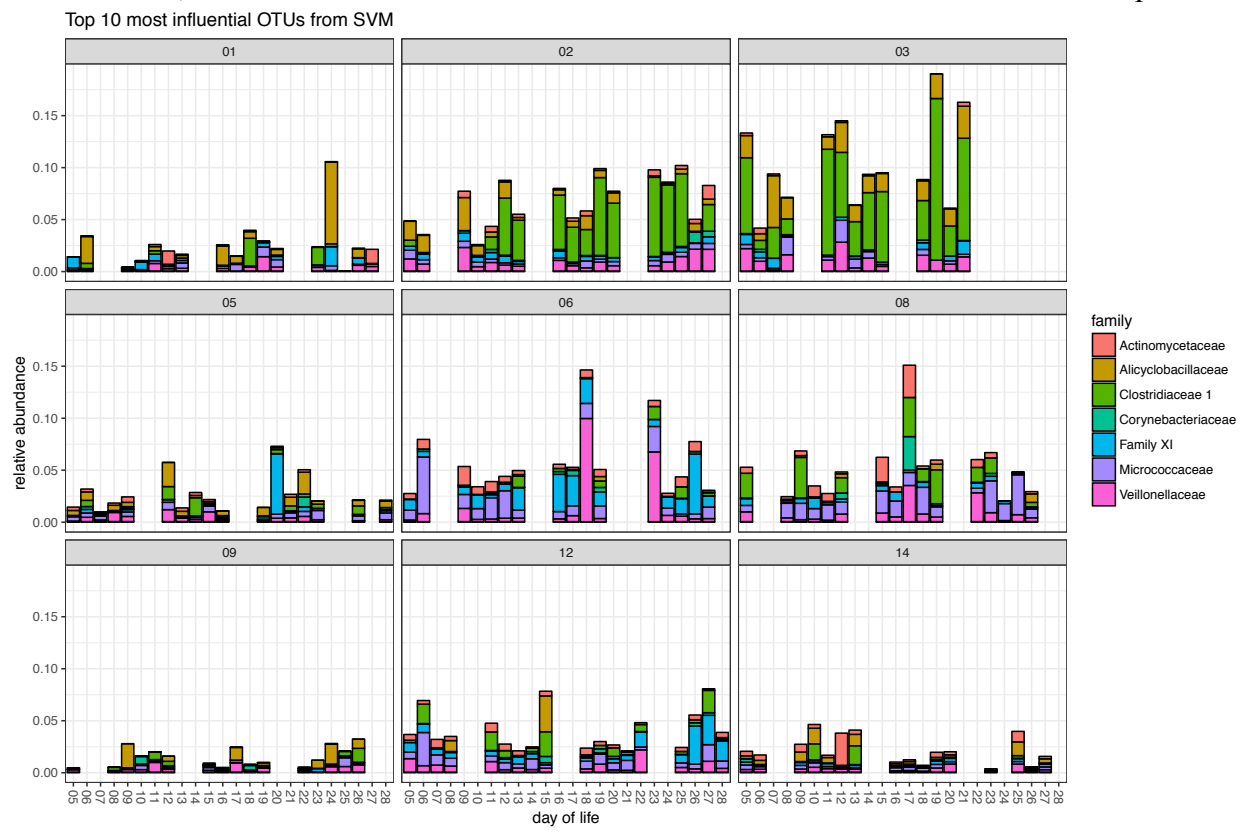
682  
 683  
 684

685 Additional file 5: **Alpha diversity in a NICU.** 16S rRNA amplicon data was used to calculate  
 686 number of OTUs per environment (a) and the Shannon diversity (b).



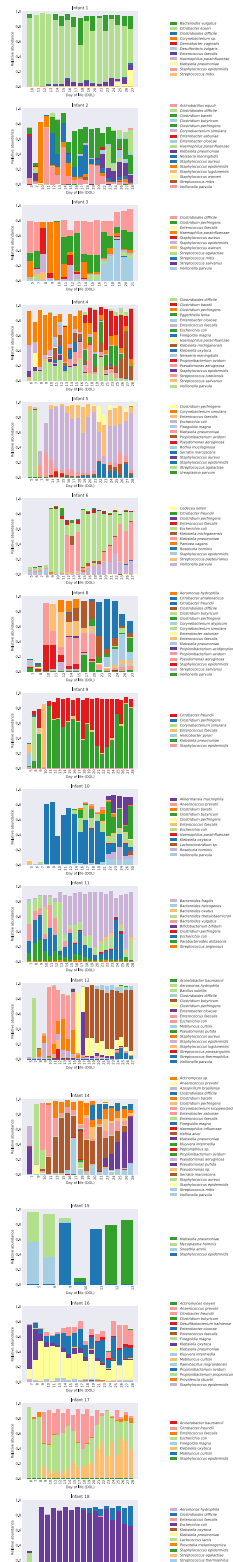
687  
 688  
 689

690 Additional file 6: **Top 10 most important taxa driving the machine learning model.** The top  
 691 10 most important variables driving the SVM model are plotted for each infant. On the y-axis,  
 692 “Abundance”, notes the relative importance.



693  
 694  
 695

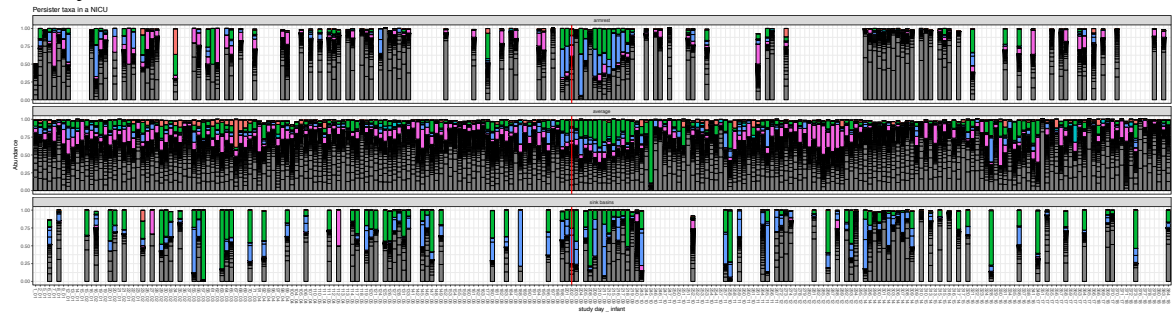
696 Additional file 7: **Fecal sample community composition**. Plotted in each panel is the community  
697 composition of each infant's fecal samples derived from metagenomics data.



698

699

700 Additional file 8: **Episodic increases in persistent taxa.** The “average” panel represents 16S  
701 amplicon data averaged across all samples at each time point per infant. The “armrest” and  
702 “sink\_basins” panel is the same data but without averaging across environments. The red line  
703 highlights the time point in which an increase of *Enterobacteriaceae* was detected in infant 9’s  
704 gut. Samples are plotted in chronological order on the x-axis. The plot is split across two pages for  
705 clarity.



706

707 **Table 1: Top 10 OTUs in the NICU**

OTU	Kingdom	Phylum	Class	Order	Family	Genus	Species	% Abundance
OTU_5	Bacteria	Proteobacteria	Gammaproteobacteria	Enterobacteriales	Enterobacteriaceae	Klebsiella	?	12.9
OTU_6	Bacteria	Firmicutes	Bacilli	Bacillales	Staphylococcaceae	Staphylococcus	?	7.3
OTU_4	Bacteria	Actinobacteria	Actinobacteria	Corynebacteriales	Corynebacteriaceae	Corynebacterium	?	7.1
OTU_7	Bacteria	Firmicutes	Bacilli	Lactobacillales	Streptococcaceae	Streptococcus	?	6.9
OTU_9	Bacteria	Proteobacteria	Gammaproteobacteria	Aeromonadales	Aeromonadaceae	Aeromonas	?	6.9
OTU_10	Bacteria	Proteobacteria	Alphaproteobacteria	Rhizobiales	Rhizobiaceae	Rhizobium	?	4.5
OTU_8	Bacteria	Proteobacteria	Gammaproteobacteria	Pseudomonadales	Pseudomonadaceae	Pseudomonas	?	3.7
OTU_11	Bacteria	Proteobacteria	Gammaproteobacteria	Pseudomonadales	Moraxellaceae	Acinetobacter	?	2.3
OTU_30	Bacteria	Firmicutes	Clostridia	Clostridiales	Clostridiaceae 1	Clostridium sensu stricto 1	?	1.9
OTU_32	Bacteria	Proteobacteria	Alphaproteobacteria	Caulobacterales	Caulobacteraceae	Brevundimonas	?	1.8

708

709

710 **Table 2: Most important variables to SVM model**

711

OTU	Kingdom	Phylum	Class	Order	Family	Genus	Species
OTU_29	Bacteria	Firmicutes	Clostridia	Clostridiales	Clostridiaceae 1	<i>Clostridium sunsu</i> <i>stricto</i> 1	uncultured organism
OTU_39	Bacteria	Actinobacteria	Actinobacteria	Micrococcales	Micrococcaceae	<i>Rothia</i>	uncultured organism
OTU_41	Bacteria	Firmicutes	Bacilli	Bacillales	Family XI	<i>Gemella</i>	?
OTU_30	Bacteria	Actinobacteria	Actinobacteria	Micrococcales	Micrococcaceae	<i>Kocuria</i>	?
OTU_45	Bacteria	Actinobacteria	Actinobacteria	Actinomycetales	Actinomycetaceae	<i>Actinomyces</i>	?
OTU_43	Bacteria	Firmicutes	Bacilli	Bacillales	Alicyclobacillacea e	<i>Tumebacillus</i>	uncultured Firmicutes bacterium
OTU_76	Bacteria	Firmicutes	Clostridia	Clostridiales	Family XI	<i>Peptoniphilus</i>	?
OTU_74	Bacteria	Actinobacteria	Actinobacteria	Actinomycetales	Actinomycetaceae	<i>Actinomyces</i>	uncultured organism
OTU_28	Bacteria	Firmicutes	Negativicutes	Selenomonadale s	Veillonellaceae	<i>Veillonella</i>	uncultured organism
OTU_66	Bacteria	Firmicutes	Bacilli	Lactobacillales	Streptococcaceae	<i>Streptococcus</i>	?

712